BBA - Bioenergetics 1865 (2024) 149043

Contents lists available at ScienceDirect

BBA - Bioenergetics

journal homepage: www.elsevier.com/locate/bbabio

Elements of the C-terminal tail of a C-terminal domain homolog of the Orange Carotenoid Protein determining xanthophyll uptake from liposomes

Kristina Likkei [a], Marcus Moldenhauer [a], Neslihan N. Tavraz [a], Nikita A. Egorkin [b,c], Yury B. Slonimskiy [b], Eugene G. Maksimov [c], Nikolai N. Sluchanko [b], Thomas Friedrich [a,*]

[a] Technische Universität Berlin, Institute of Chemistry, PC 14, Straße des 17. Juni 135, 10623 Berlin, Germany
[b] Federal Research Center of Biotechnology of the Russian Academy of Sciences, A.N. Bach Institute of Biochemistry, Leninsky Prospect 33-1, Moscow 119071, Russian Federation
[c] Lomonosov Moscow State University, Faculty of Biology, Leninskie Gory 1-12, Moscow 119991, Russian Federation

ARTICLE INFO

Keywords:
Orange Carotenoid Protein
CTDH protein
Carotenoid transfer
Xanthophylls
Echinenone
Canthaxanthin
Liposomes
CTT

ABSTRACT

Carotenoids perform multifaceted roles in life ranging from coloration over light harvesting to photoprotection. The Orange Carotenoid Protein (OCP), a light-driven photoswitch involved in cyanobacterial photoprotection, accommodates a ketocarotenoid vital for its function. OCP extracts its ketocarotenoid directly from membranes, or accepts it from homologs of its C-terminal domain (CTDH). The CTDH from *Anabaena* (AnaCTDH) was shown to be important for carotenoid transfer and delivery from/to membranes. The C-terminal tail of AnaCTDH is a critical structural element likely serving as a gatekeeper and facilitator of carotenoid uptake from membranes. We investigated the impact of amino acid substitutions within the AnaCTDH-CTT on echinenone and canthaxanthin uptake from DOPC and DMPG liposomes. The transfer rate was uniformly reduced for substitutions of Arg-137 and Arg-138 to Gln or Ala, and depended on the lipid type, indicating a weaker interaction particularly with the lipid head group. Our results further suggest that Glu-132 has a membrane-anchoring effect on the PC lipids, specifically at the choline motif as inferred from the strongly different effects of the CTT variants on the extraction from the two liposome types. The substitution of Pro-130 by Gly suggests that the CTT is perpendicular to both the membrane and the main AnaCTDH protein during carotenoid extraction. Finally, the simultaneous mutation of Leu-133, Leu-134 and Leu-136 for alanines showed that the hydrophobicity of the CTT is crucial for carotenoid uptake. Since some substitutions accelerated carotenoid transfer into AnaCTDH while others slowed it down, carotenoprotein properties can be engineered toward the requirements of applications.

1. Introduction

Carotenoids, a widely distributed class of pigments, are produced in plants, algae, fungi and bacteria (e.g. cyanobacteria) and serve diverse biological purposes in nature [1]. For example, they act as precursors of visual pigments, vitamins, and hormones. Due to their anti-inflammatory and antioxidant effects, they have shown promising therapeutic potential for multiple diseases, including neurodegenerative and cardiovascular disorders. Carotenoids have also demonstrated antitumor effects [2–4]. Furthermore, they have the ability to protect against reactive oxygen species (ROS) and contribute to light protection and light harvesting in photosynthesis. As a result, carotenoids frequently act as ligands in photosynthetic light-harvesting antennae and reaction centres [5–7]. Another important contribution to photosynthesis is made by water-soluble carotenoid-binding proteins expressed by cyanobacteria, from which the Orange Carotenoid Protein (OCP) is one of the most well-known. OCP diminishes the excitation in reaction centres of photosystem II during a non-photochemical

Abbreviations: AnaCTDH, C-terminal domain homolog from *Anabaena* (*Nostoc* sp.) sp. PCC 7120; CAN, canthaxanthin; CTD, C-terminal domain; CTT, C-terminal tail; DMPG, 14:0 PG – 1,2-dimyristoyl-*sn*-glycero-3-phospho-(1′-rac-glycerol); DOPC, 18:1(Δ9-Cis)PC – 18:1 PC – 1,2-dioleoyl-*sn*-glycero-3-phosphocholine; ECN, echinenone; FRP, Fluorescence Recovery Protein; HCP, helical carotenoid protein; NPQ, non-photochemical quenching; NTD, N-terminal domain; NTE, N-terminal extension; OCP, Orange Carotenoid Protein; PBS, phycobilisomes; PC, phosphatidylcholine; PG, phosphatidylglycerol; RCP, Red Carotenoid Protein; ROS, reactive oxygen species.

* Corresponding author.
E-mail address: friedrich@chem.tu-berlin.de (T. Friedrich).

https://doi.org/10.1016/j.bbabio.2024.149043
Received 6 December 2023; Received in revised form 7 March 2024; Accepted 9 March 2024
Available online 23 March 2024

quenching (NPQ) process, thus preventing ROS formation and oxidative damage under intense light exposure, and its function has been extensively studied [8–11].

OCP, e.g. from *Synechocystis* sp. PCC 6803, is a 35 kDa water-soluble protein that is photoactive and consists of two structural domains, the N-terminal domain (NTD) and the C-terminal domain (CTD), connected by a flexible linker [12,13]. In the dark, OCP exists in the inactive orange state OCP^O and the two main domains of OCP enclose a keto-carotenoid as a cofactor within a shared central cavity. This keto-carotenoid, specifically the xanthophylls 4-monoketolated echinenone (ECN) and 3′-hydroxyechinenone, or 4,4′-diketolated canthaxanthin (CAN), imparts photoactivity to OCP [13–15]. The presence of the 4-keto group is essential for the specific carotenoid-protein interactions via hydrogen bonds between the keto group of the carotenoid and two amino acids of the CTD (Tyr-201 and Trp-288 in *Synechocystis* OCP) [16]. This inactive state OCP^O is stabilized by the N-terminal extension (NTE) of the NTD interacting with the CTD, while the C-terminal tail (CTT) binds to the CTD (Fig. 1A). In intense light, the OCP transitions to the active red state OCP^R. As a result of photon absorption, hydrogen bonds between the CTD and the carotenoid become unstable and prompt a 12 Å carotenoid translocation into the NTD, which triggers subsequent steps causing substantial conformational changes. These processes ultimately interrupt the NTE-CTD interaction, fully separating the carotenoid-binding NTD from the carotenoid-free CTD, connected only by the flexible loop [17–21]. In this active state, OCP^R interacts with the phycobilisomes (PBS), the cyanobacterial light-harvesting antennae, through the carotenoid-containing NTD. This interaction causes structural changes in the PBS complex that prevent the transfer of excess excitation energy, in effect protecting the photosystems from photodestruction. The physiological interaction partner of OCP, the Fluorescence Recovery Protein (FRP), subsequently terminates the OCP-PBS interaction and expedites the return to the OCP^O state [22–25].

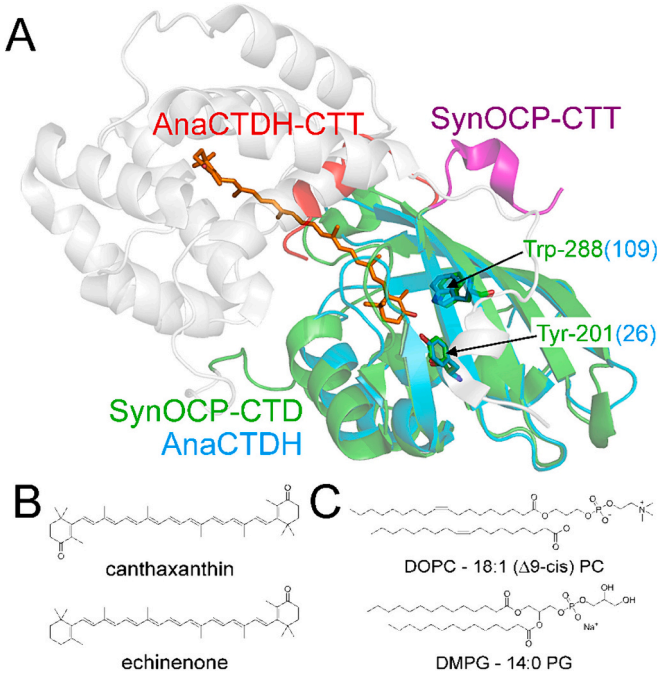

Fig. 1. Structural overview of *Synechocystis* OCP and AnaCTDH and molecular structure of lipids and carotenoids used in this study. (A) Structural alignment of the C-terminal domain of *Synechocystis* OCP (green, PDB ID 4XB5) and AnaCTDH (cyan, PDB ID 6FEJ, chain A) prepared with PyMol 2.5.5. The OCP-CTT is shown in violet, the carotenoid cofactor of OCP (canthaxantin in PDB ID 4XB5) in orange, the CTT of AnaCTDH in red, and the OCP-NTD is indicated in light grey. Also shown in ball-and-stick representation are the OCP residues Tyr-201 and Trp-288 (Tyr-26 and Trp-109 in AnaCTDH), which form hydrogen bonds to the ketocarotenoid. (B) Carotenoids used for transfer experiments: canthaxanthin (CAN) and echinenone (ECN). (C) Lipids used for liposome preparation: DOPC and DMPG.

The sequencing of cyanobacterial genomes has led to the identification of new protein families that share homology with the main domains of OCP. So far, nine clades of NTD homologs have been discovered and named helical carotenoid proteins (HCP, HCP1-HCP9) due to their solely α-helical structure [26–28]. Some of them have the ability to directly quench electronic excitation of pigments from light-harvesting antennae and/or singlet oxygen as does the isolated OCP-NTD, formerly known as the Red Carotenoid Protein (RCP) [26–29]. In contrast, only two clades of CTD homologs have been identified (CTDH1 and CTDH2), which belong to the widely distributed class of nuclear transport factor 2 (NTF2)-like proteins, termed either C-terminal domain homologs (CTDH) or C-terminal domain-like carotenoid proteins (CCP) [30,31]. A thoroughly investigated CTDH protein is that of the cyanobacterium *Anabaena* sp. PCC 7120, commonly referred to as AnaCTDH [26,30,32]. AnaCTDH could be crystallized and its structure solved only for two apoprotein oligomers [31]. According to the crystal structures and further NMR- and SAXS-based analyses [32,33], the CTDH has an overall structural organization very similar to that of the OCP-CTD and has remarkable dynamics of several loops and the CTT, which is thought to be a functionally relevant element (Fig. 1A). Besides AnaCTDH, only the CTDHs from *Thermosynechococcus elongatus* and *Fremyella diplosiphon* were studied, but less comprehensively [30,32,34]. Very little is known about CTDHs from other cyanobacteria and about their distant homologs with unknown function. Of note, there is an X-ray crystal structure of a structural analogue of CTDH proteins deposited in the Protein Data Bank (PDB ID 5TGN), which belongs to a SnoaL-like domain-containing protein (SLDCP; Uniprot D1C7H4); however, this protein has not yet been analyzed regarding its function or carotenoid-binding properties.

Recent studies have shown that both CTDH and the isolated OCP-CTD function as ROS quenchers while also serving as an efficient platform for carotenoid uptake, storage, and delivery [30,35,36]. Ketocarotenoids, such as echinenone (ECN) and canthaxanthin (CAN), can be extracted by these proteins from membranes of carotenoid-producing *E. coli* strains as well as from artificial liposomes [30,34–36]. Investigations using liposomes consisting of defined lipids with different physicochemical properties demonstrated that the uptake by the AnaCTDH is also affected by the composition of the liposomes [37]. Furthermore, carotenoid uptake also occurs through protein-protein interaction, for example, from HCP1, the only NTD homolog from *Anabaena* lacking the ability to quench excitation energy transfer or ROS, or from the activated OCP^R state. This allows the subsequent transfer of the carotenoids to other HCPs or OCP, resulting in the formation of photoactive proteins [34,35]. Even the delivery of carotenoids into mammalian cell membranes was achievable using AnaCTDH as a shuttle system [30,31,34,36,38]. According to current assumptions, CTDH proteins exist predominantly as a homodimer during these processes and undergo a reorganisation from the 'back-to-back' dimerizing apoform, which extracts the carotenoid, to the 'head-to-head' dimerizing holoform, which encapsulates the bound CAN molecule until release. However, when ECN is incorporated, the holoprotein AnaCTDH(ECN) appears at the end as both a monomer and a dimer. The absence of the second keto group in ECN is responsible for the lack of carotenoid-protein interaction on one side of the molecule, which in turn leads to a less stable dimer [30,31,34,39].

The CTT of OCP has been implicated in characteristic structural changes occurring upon photoexcitation of OCP. Results from transient UV–Vis and mid-IR absorption spectroscopy studies suggested that structural changes of internal (non-solvent-exposed) α-helical elements occur early after photoexcitation, while structural changes of α-helical elements assigned to the NTE and the CTT occur later [40,41]. Since the CTT assumes different positions in the structure of dark-adapted OCP and in the *Anabaena* CTDH apoprotein, it is likely that the CTT

conformational change is a late event, which is only possible after the separation of NTD and CTD, and that the CTT serves as a lid to control access to the carotenoid-coordinating tunnel [31]. The nonlinear response of OCP to pulsed or continuous light has recently prompted the notion of a two-photon activation mechanism of OCP [42,43], and it is well conceivable that the CTT conformational change is correlated to the second photon absorption event. But, the CTT plays a crucial role in the transfer of carotenoids, as demonstrated by the marked decrease in carotenoid uptake and subsequent production of AnaCTDH holoprotein when utilizing protein variants lacking the CTT. The crystal structure and molecular dynamics simulations of AnaCTDH offered valuable insight into the dynamics of the CTT and the amino acid residues that affect these dynamics [31]. First carotenoid transfer experiments based on site-directed mutagenesis provided evidence for this notion, as some CTT mutations inhibited carotenoid uptake and release [31,39]. To expand the research on the role of the CTT and our previous work on protein-lipid interaction by variation of the liposome composition, we generated a range of AnaCTDH protein variants with point mutations within the CTT region and performed carotenoid transfer experiments from chemically defined liposomes to form AnaCTDH holoprotein. In particular, we considered the polar, acidic and basic amino acids, as well as the flexibility and overall hydrophobicity of the CTT, in order to define the role of these individual amino acids or structural elements, and to gain insight into their function.

2. Materials and methods

2.1. Materials

1,2-Dioleoyl-*sn*-glycero-3-phosphocholine (DOPC, 18:1 (Δ9-Cis) PC) and 1,2-dimyristoyl-*sn*-glycero-3-phospho-(1′-*rac*-glycerol) (sodium salt) (DMPG, 14:0 PG) were obtained from Avanti Polar Lipids Inc. (USA).

2.2. Carotenoid production and extraction

Echinenone (ECN) production in *E. coli* cells was accomplished based on the p25crtO plasmid, which comprises the contiguous gene cluster harboring the genes *crtY*, *crtI*, *crtB*, and *crtE* from *Pantoea ananatis* (formerly *Erwinia uredovora*) and the *crtO* gene from *Synechocystis* sp. PCC 6803, as described previously [44]. For the predominant production of canthaxanthin (CAN) in *E. coli*, the cDNA of the β-carotene biketolase of *Chlamydomonas reinhardtii* (crBKT) was subcloned into the position of the *crtO* monoketolase gene in p25crtO by recombinant PCR, as reported before [37]. After transformation into BL21(DE3) *E. coli* cells (New England Biolabs), carotenoid production and extraction were carried out as previously described. Briefly, both carotenoids were produced in *E. coli* cells cultivated in LB medium supplemented with chloramphenicol, subsequently extracted with a mixture of acetone and methanol, and purified by flash chromatography (silica gel, acetone: hexane (1:6, v/v)). CAN and ECN were identified by thin-layer chromatography [45] and mass spectrometry (APCI, Orbitrap XL, Thermo Fischer Scientific, USA).

2.3. Protein expression and purification

The construct of the plasmid containing the C-terminal domain homolog from *Anabaena* (*Nostoc* sp.) PCC 7120 (AnaCTDH) was previously described [37]. Of note, numbering of the AnaCTDH amino acids in the present work follows the sequence of the *all4940* gene of *Anabaena* (*Nostoc*) sp. PCC 7120 (UniProt entry Q8YMJ3) and differs from the numbering used in PDB entry 6FEJ, which is sometimes referred to in the literature. The point mutations E132A, E132Q, R137A, R137Q, R138A, R138Q, P130G and the triple leucine mutation L133A/L134A/L136A (termed 3LA herein) were introduced by site-directed mutagenesis with the Q5 site-directed mutagenesis kit (New England Biolabs), using the pRSFDuetN-AnaCTDH plasmid as template and mismatching primers (Supplementary information, Table S1) designed by using NEBaseChanger online tool and synthesized by Merck KgA (Darmstadt, Germany) and LGC Genomics (Berlin, Germany). All cDNA sequences obtained in this way were verified by sequencing (LGC Genomics, Berlin). For the expression of the AnaCTDH apoprotein and variants, the plasmids harboring the cDNAs of the AnaCTDH constructs were transformed into BL21(DE3) *E. coli* cells. The expression conditions and purification were described earlier [46,47]. All 6 × His-tagged apoproteins were expressed in LB medium supplemented with kanamycin upon induction with isopropyl *β-D*-1-thiogalactopyranoside (IPTG). For protein purification, immobilized metal ion affinity chromatography (IMAC) was performed, and all proteins were stored in phosphate buffer (PBS: 137 mM NaCl, 2.7 mM KCl, 10 mM Na_2HPO_4, 2 mM KH_2PO_4, pH 7.4) at −80 °C until use.

The cDNA of SnoaL-like domain-containing protein (SLDCP; Uniprot D1C7H4) was synthesized by IDT DNA technologies (Coralville, USA) and cloned in-house into the pET28 vector using *Nde*I and *Xho*I sites so that extra residues GSH would be present at the N-terminus of the protein after thrombin cleavage. The correctness of the obtained construct was verified by DNA sequencing (Evrogen, Moscow, Russia). In order to test the carotenoid-binding capacity, AnaCTDH or SLDCP were expressed in *E. coli* cells synthesizing echinenone and canthaxanthin [44] and were purified by subtractive IMAC and size-exclusion chromatography (SEC) as described previously [34]. Performing SEC of SLDCP, we observed a small dimeric and a major monomeric protein peaks both devoid of any absorbance in the visible spectral region, and the fractions of the monomeric protein peak were pooled together for further analysis by small-angle X-ray scattering (SAXS).

2.4. Production of carotenoid-loaded liposomes

Carotenoid-loaded liposomes were prepared by thin-film evaporation and extrusion method as described earlier [37,48,49]. Briefly, the respective carotenoids and lipids were dissolved in organic solvents together, and after evaporation, the resulting thin film was dried under vacuum overnight, followed by hydration with phosphate buffer for 1 h at 30 °C. The lipid concentration in the liposomal suspension was around 2.2 mM and the initial concentration of carotenoids was 0.1 mol-%. For preparation of unilamellar liposomes, the suspension was extruded 25 times through a polycarbonate filter with an average pore diameter of 0.1 μm (Whatman plc, UK; Avanti Polar Lipids, USA) and the resulting liposomes were stored in the dark at 4 °C under argon atmosphere until use.

2.5. Absorption measurements

2.5.1. Carotenoid and protein concentration

For the calculation of the carotenoid concentration, the absorption spectra of the carotenoids extracted from the membranes of the ECN/CAN-producing *E. coli* cells and the carotenoids extracted from the liposomes with ethanol were recorded on a Maya2000 Pro spectrometer (Ocean Optics, USA) and the molar absorption coefficients reported in the literature were used for concentration determination [50]. Protein concentration was determined spectrophotometrically from the absorbance at 280 nm using the protein-specific molar extinction coefficient 15,470 M^{-1} cm^{-1} for AnaCTDH and 13,980 M^{-1} cm^{-1} for SLPCD, calculated using the ExPASy ProtParam tool, and the holoprotein concentration was additionally determined by visible-to-UV absorbance ratio ($A_{550\ nm}/A_{280\ nm}$), and from the extinction coefficient resulting in turn.

2.5.2. Carotenoid-to-protein transfer kinetics and transfer yield

Measurements of steady-state absorbance spectra and the time courses of absorbance changes were performed using a Maya2000 Pro spectrometer (Ocean Optics, USA), and the sample temperature was

stabilized by a Peltier-controlled cuvette holder Qpod 2e (Quantum Northwest, USA). The kinetics of CAN transfer was measured with a time resolution of 100 ms as the change of optical density at 550 nm. The molecular carotenoid-to-apoprotein ratio used was 1:50. Therefore, the AnaCTDH apoprotein was consistently present in a significant excess. CAN transfer was performed for 3 h at 30 °C and for ECN transfer, the sample was incubated for additional 21 h at room temperature (total incubation time 24 h) until measurement. The kinetic characteristics of the CAN transfer were determined by approximation of the measured data by a biexponential function. Subsequently, the apparent rate constant k_{app} was calculated using the following equations.

$$\tau_{app} = \frac{(A_1 \cdot \tau_1) + (A_2 \cdot \tau_2)}{A_1 + A_2} \quad (1)$$

$$k_{app} = \frac{1}{\tau_{app}} \quad (2)$$

The rate constant for each variant was determined by performing the experiments twice using the same protein preparation, but with distinct, freshly prepared liposome preparations (technical replicates).

The determination of the transfer yield was carried out as described previously [37]. Briefly, the absorbance spectrum of the transfer product was first corrected to remove the Rayleigh scattering background. Subsequently, the background-corrected spectrum was decomposed into a fractional contribution of the initial absorbance spectrum of the CAN/ECN-loaded liposome preparation and a fraction corresponding to the spectrum of CAN/ECN-containing AnaCTDH holoprotein, which was supposed to represent the transfer yield of the wild-type and the mutants. ECN transfer yields of specific mutants were analyzed for significance using the unpaired *t*-test with a significance threshold of $p < 0.05$. The transfer yield for each variant was determined by performing the experiments three times using the same protein preparation, but distinct, freshly prepared liposome preparations (technical replicates).

2.6. Small-angle X-ray scattering

SAXS data ($I(s)$ against s, where $s = 4\pi \sin\theta/\lambda$, 2θ is the scattering angle and $\lambda = 1.24$ Å) were collected from a concentration series of SLDCP protein samples (1.43, 3.57, 6.59, 11.48 mg/mL) produced by gradual concentration of the fractions derived from the monomeric SEC peak. The measurements were done at 20 °C at the EMBL P12 beam line (PETRA III, DESY Hamburg, Germany) using a batch mode (1 s exposure time, collected as 20 × 50 ms frames), in 20 mM Tris-HCl buffer (pH 7.6) containing 150 mM NaCl, 0.1 mM EDTA, 2 mM DTT, and 3 % v/v glycerol. SAXS data processing in PRIMUS was done as described earlier [51]. The resulting curve was produced by scaling and merging of the low and high protein concentration SAXS curves according to the widely accepted approaches. The CRYSOL program [52] was used for fitting of the SAXS data by the SLDCP monomer (PDB ID: 5TGN, chain A) or the AnaCTDH monomer (PDB ID: 6FEJ, chain B) as is. Approximation of the SAXS data by crystallographic oligomers of SLDCP (dimer, trimer, tetramer) produced inadequate fits ($\chi^2 > 5$). The SAXS data and fitting model for the SLDCP apoprotein have been deposited in the SASBDB database (code SASDTT4).

3. Results and discussion

3.1. AnaCTDH and its homolog with the analogous structure markedly differ by the carotenoid-binding capacity

It was previously shown that AnaCTDH can efficiently extract the carotenoids canthaxanthin (CAN) and echinenone (ECN) (Fig. 1B) from membranes of carotenoid-producing *E. coli* strains [30,34] as well as from artificial liposomes [36,37]. Studies of saturated and unsaturated phosphatidylglycerol and phosphatidylcholine lipids revealed that liposomes composed of DOPC (18:1 (Δ9-cis) PC) and DMPG (14:0 PG) lipids (Fig. 1C) are best suited to form AnaCTDH(CAN) and AnaCTDH (ECN) holoproteins by carotenoid transfer from liposomes at 30 °C, thus setting the best conditions for further investigations of the lipid-protein interaction and the carotenoid uptake process from lipid membranes. Previous studies already suggested that the C-terminal tail (CTT) of AnaCTDH (amino acid sequence 126-LLASPQELLALRREQ-COOH, Fig. 2A, B) may be a critical determinant for the interaction of AnaCTDH with lipid membranes, since it could be shown that carotenoid uptake from membranes is largely reduced upon removal of the CTT structural element, i.e. only 20 % of the holoprotein was produced instead of about 100 % in the case of non-truncated AnaCTDH [31,39].

We asked whether the carotenoid-binding capacity is associated with the protein fold characteristic of AnaCTDH and its CTT. Since no structure of a CTDH protein from other cyanobacteria has been reported to date, we searched for more distant homologs and found a SnoaL-like domain-containing protein (SLDCP) from the green non-sulfur bacterium *Sphaerobacter thermophilus* (see Fig. 2A for a sequence alignment with *Synechocystis* OCP and AnaCTDH), whose unliganded crystal structure is well superimposable with that of AnaCTDH (Cα RMSD of <1 Å) including the conserved Tyr and Trp residues known to form hydrogen bonds to the ketocarotenoid in AnaCTDH (Fig. 2B, C). The similarity of the monomer fold of these proteins could be directly confirmed by SAXS data collected for recombinant SLDCP in solution, as these data could be nearly equally well described by the crystallographic monomers of SLDCP or AnaCTDH (Fig. 2D). Nevertheless, we noted that the CTT in SLDCP is extremely short (Fig. 2A, B, C). Intriguingly, in contrast to AnaCTDH, when SLDCP was produced in the ketocarotenoid-synthesizing *E. coli* cells we failed to detect any carotenoid binding, as the purified protein was colorless even at high protein concentration (11.4 mg/mL). This indicated that, despite the presence of the conserved carotenoid-coordinating Tyr/Trp residues, the preservation of the CTDH-like protein fold is not sufficient for efficient carotenoid binding, indirectly supporting the role for the CTT in this process.

3.2. Selection of AnaCTDH CTT mutants

To further investigate the role of individual amino acids relating to their physical or chemical properties in functioning of the CTT in AnaCTDH, we generated several AnaCTDH variants carrying point mutations in the CTT region (amino acid numbering according to sequence of the *all4940* gene of *Anabaena* (*Nostoc*) sp. PCC 7120 (UniProt entry Q8YMJ3)) [31]. The amino acids Glu-132 and Arg-137 were suggested to exert an anchoring effect at the membrane [36]. Therefore, these two charged amino acids and the subsequent Arg-138 were mutated to Ala and Gln to analyze whether and how carotenoid uptake was affected by neutralizing the charge of the side chain or – in addition – reducing the length of the side chain. The following AnaCTDH mutants were generated: E132A, E132Q, R137A, R137Q, R138A and R138Q (Figs. 2A and 3A). Apart from the polar acidic/basic amino acids, the hydrophobic leucines (Leu-133, Leu-134, and Leu-136) within the α-helical region of the CTT were also considered and simultaneously replaced by alanines for investigating the influence of a reduction in hydrophobicity of this region on carotenoid transfer (the resulting AnaCTDH mutant was termed 3LA) [53]. Another amino acid of interest was Pro-130, which is located between the α-helical structure and the hinge region of the CTT (Ala-128 and Ser-129), thereby putatively serving a critical role to allow for rotation of the CTT between the closed and open conformation [39]. Pro-130 was mutated to a glycine to observe the impact of a change in flexibility of the CTT region while preserving the helix-breaker function [54] (resulting AnaCTDH mutant termed P130G). Carotenoid transfer experiments were performed with all AnaCTDH sequence variants and the wild-type protein into which CAN and ECN were transferred from DMPG and DOPC liposomes at 30 °C. The effect of the mutations on the kinetic characteristics and transfer yield of AnaCTDH holoprotein was monitored by absorption spectroscopy.

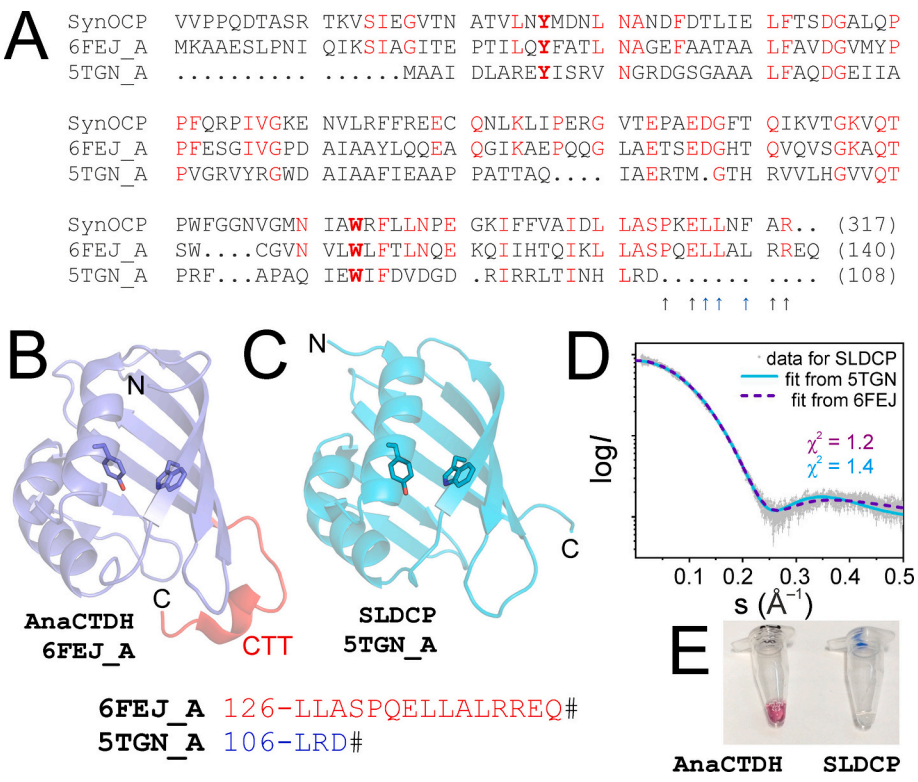

Fig. 2. Comparison of AnaCTDH and its distant homolog, SnoaL-like domain-containing protein (SLDCP) in terms of sequence, structure and carotenoid-binding capacity. (A) Sequence alignment of *Synechocystis* OCP-CTD, AnaCTDH (PDB ID 6FEJ, chain A) and SLDCP (PDB ID 5TGN, chain A). Residues conserved between OCP-CTD and CTDH sequences (according to the analysis performed by Muzzopappa et al. [30]) are shown in red, identical residues on the SLDCP sequence are also shown in red. The conserved Trp and Tyr residues (Tyr-201 and Trp-288 in OCP, Tyr-10 and Trp-89 in SLDCP, Tyr-26 and Trp-109 in AnaCTDH), which form hydrogen bonds to the ketocarotenoid, are indicated in bold red. Amino acids within the AnaCTDH-CTT mutated in this work are indicated by arrows. (B) Crystal structure of AnaCTDH in the apoform (PDB ID 6FEJ, chain A). (C) Crystal structure of SLDCP in the apoform (PDB ID 5TGN, chain A). Note the presence of the CTT in AnaCTDH only. The two conserved residues Tyr-26 and Trp-109 forming hydrogen bonds to the ketocarotenoid in AnaCTDH (B) and the homologous residues Tyr-10 and Trp-89 in SLDCP (C) are shown as sticks. The sequences of the C-terminal tails of the two proteins are shown below. (D) Structural similarity of the two protein monomers is verified by small-angle X-ray scattering (SAXS) in solution. The data obtained for SLDCP are fitted by either SLDCP or AnaCTDH monomer models. The quality of the fits is represented by χ^2 values indicated. (E) Unlike AnaCTDH, SLDCP is not able to extract ketocarotenoid from membranes of *E. coli* cells synthesizing echinenone and canthaxanthin. The appearance of the final purified protein samples is shown.

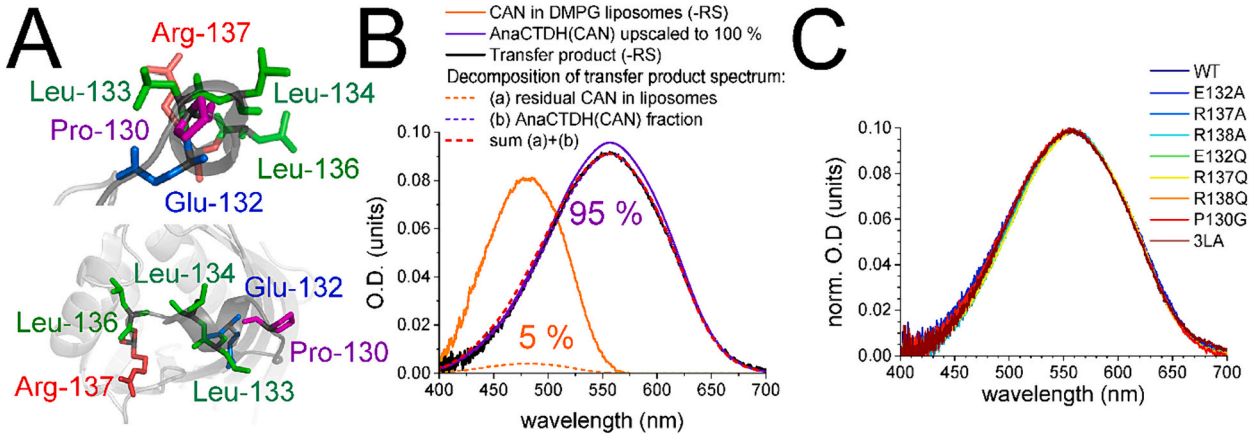

Fig. 3. CTT structure and CAN uptake by AnaCTDH apoprotein and variants thereof from artificial liposomes exemplified by DMPG liposomes. (A) – Structure of the CTT of AnaCTDH (PDB 6FEJ, numbering according to sequence of the *all4940 gene* (see method section)) viewed along the α-helix (upper panel) and from top (lower panel) with amino acids mutated in this study in ball-and-stick representation. Note that the three C-terminal amino acids including Arg-138 are missing in the 6FEJ structure. (B) – Typical absorption spectrum of CAN in DMPG liposomes (solid orange line) and of the transfer product (black line) measured after addition of an excess of AnaCTDH wild-type apoprotein and incubation at 30 °C until transfer was completed (max. 3 h). The spectra shown were obtained after subtraction of the Rayleigh scattering background (-RS). For analysis, the transfer product spectrum was decomposed into a fraction of the CAN-loaded liposome preparation ((a), dashed orange line, here 5 %) and a fraction corresponding to the CAN-containing AnaCTDH holoprotein spectrum ((b), dashed purple line, here 95 %). The sum of the two fractions (a) and (b) are shown as a dotted red line and a spectrum of the AnaCTDH(CAN) holoprotein corresponding to a transfer yield of 100 % is shown as a solid purple line. (C) – Exemplary normalized absorption spectra of the transfer products of AnaCTDH wild-type and all variants obtained by CAN transfer at 30 °C from DMPG liposomes after completion of the transfer and Rayleigh scattering background correction.

3.3. Influence of point mutations in the CTT region of AnaCTDH on canthaxanthin uptake

CAN transfer from liposomes into AnaCTDH to form the AnaCTDH (CAN) holoprotein was detected spectroscopically by monitoring the change in absorbance at 550 nm (Fig. 3B) [31,34,37]. The absorbance spectra of the holoproteins after transfer were essentially identical for all AnaCTDH variants and the wild-type (WT) protein (Fig. 3C) (except for the slightly varying minor fraction of remaining CAN-loaded liposomes), indicating that the carotenoid-protein interaction in all investigated AnaCTDH variants is similar.

None of the AnaCTDH sequence variants studied revealed a significant effect on the transfer yield of AnaCTDH(CAN) holoprotein from DMPG and DOPC liposomes compared to AnaCTDH wild-type (Table 1). Namely, within 3 h at 30 °C, nearly all CAN molecules (89–95 %) were extracted by an excess of apoprotein.

The kinetic characteristics of carotenoid uptake from liposomes were determined spectroscopically by monitoring the absorbance change at 550 nm. The CAN transfer rate from DMPG liposomes into the AnaCTDH wild-type protein was only slightly faster ($[2.69 \pm 0.08]\cdot10^{-3}$ s^{-1}) than from DOPC liposomes ($[2.05 \pm 0.40]\cdot10^{-3}$ s^{-1}) (Table 1, Fig. 4), as demonstrated previously [37]. Due to the similar rate constant despite the different lipid head groups, these lipids are very suitable for studying the lipid-protein interaction between the various AnaCTDH variants because of presenting two types of head groups: negatively charged for DMPG and zwitterionic for DOPC. In contrast to the transfer yield, the mutations within the CTT region of AnaCTDH had an influence on the transfer rate compared to the one of AnaCTDH wild-type (Table 1, Fig. 4). All arginine mutants exhibited slower CAN uptake compared to the wild-type protein (Fig. 4A, B, D and E). Furthermore, all constructs performed almost identically in terms of transfer kinetics depending on the liposome type (Fig. 5A, Table 1). Each of these mutations most probably resulted in a weaker interaction of the CTT with the liposome, especially with the head group, and, consequently, in a decreased transfer rate with equal intensity within the liposome type. Thus, it was irrelevant which arginine (Arg-137 or Arg-138) was replaced or by which amino acid (Gln or Ala) it was substituted because the effect was almost equal. Therefore, no superior role for Arg-137 over Arg-138 as, e.g., membrane anchor in CAN transfer could be demonstrated. However, this possibly could result from the fact that CAN transfer is generally very fast and efficient so that differences between both arginine mutants are difficult to resolve. However, comparing the two types of liposomes, the negative effects on the transfer rate were observed to be much stronger for DOPC than for DMPG liposomes. The negative total charge of the DMPG head group is possibly more suitable to compensate for the interaction with the missing positively charged arginine than the zwitterionic DOPC.

The third charged amino acid considered was Glu-132. In contrast to mutating amino acids Arg-137 and Arg-138, the substitution of Glu-132 by an alanine (Fig. 4A and D) or glutamine (Fig. 4B and E) led to different results (Table 1). In liposomes composed of zwitterionic DOPC, the E132Q mutation led to almost the same decrease in transfer rate as mutations of Arg-137/Arg-138 (Fig. 4B, Table 1). Thus, each type of charge removal had similarly strong effects on the protein-lipid interaction. In contrast, shortening the amino acid side chain to alanine (E132A) resulted in a rate constant approaching the value characteristic for the AnaCTDH wild-type protein. Possibly, compared to the E132Q mutation, steric reasons related to the shorter side chain could be of importance leading to this advantage. In CAN transfer from DMPG liposomes, the E132A mutation exhibits a slightly slower time course compared to AnaCTDH wild-type and the Arg-137/Arg-138 variants (Fig. 4D, Table 1). Direct comparison of the carotenoid uptake kinetics of the AnaCTDH-E132A construct from both liposome types shows that the time course and the apparent rate constant are identical within the error margins (Fig. 5B, Table 1). A role in anchoring to the membrane can be attributed to the Glu-132 residue in a model that assumes an interaction with the (positively charged) choline moiety of PC lipids [36]. If the replacement by an alanine would prevent any type of interaction with the choline moiety of the PC lipid or the glycerol moiety of the PG lipid, essentially the same transfer rate would result. This observation suggests that Glu-132 is important for protein-lipid interaction to bring about CAN uptake. Furthermore, CAN uptake from DMPG liposomes by the AnaCTDH-E132Q construct was strongly accelerated compared to wild-type (Fig. 4E, Table 1). The removal of the negative charge, and, most likely, removal of the repulsive interaction with the negatively charged head group can be excluded as the sole cause, since the same effect would be expected to occur with the E132A mutant. Therefore, we assume that an interaction-promoting effect occurs as a result of the E132Q exchange compared to E132A. Hydrogen bonds between the glutamine and the glycerol of the PG lipid (Fig. 5C) would be conceivable here, and would support the hypothesis of the membrane-anchoring effect of this amino acid position within the CTT, and, unlike glutamic acid (present in the wild-type sequence), there would be no negative repulsion in this scenario.

Furthermore, the effect of changing the flexibility of the CTT was investigated. The replacement of Pro-130 by a glycine in mutant P130G presumably allows for maximum increase in flexibility while preserving the helix-breaker function [54]. CAN transfer from both liposome types was faster upon the P130G mutation compared to AnaCTDH wild-type (Fig. 4C and F, Table 1). Currently, the CTT is assumed to insert perpendicularly into the membrane, also being perpendicular to the AnaCTDH globular protein, since this allows the maximum reach for

Table 1
Comparison of the transfer yields of AnaCTDH(CAN) holoprotein and the apparent rate constant for the transfer of CAN at 30 °C from DOPC and DMPG liposomes into AnaCTDH wild-type and all sequence variants studied. Results are expressed as mean value ± standard deviation, which are provided in juxtaposed columns (transfer yield: $n = 3$, apparent rate constant: $n = 2$), with the mean values depicted as bars by using the conditional formatting tool of Microsoft Excel.

Protein	Transfer yield [%]				Apparent rate constant k_{app} [$\cdot10^{-3}$ s^{-1}]			
	from DOPC liposomes		from DMPG liposomes		from DOPC liposomes		from DMPG liposomes	
	Ø	σ	Ø	σ	Ø	σ	Ø	σ
WT	93	4	95	3	2.05	0.40	2.69	0.08
E132A	93	3	91	3	1.52	0.13	1.61	0.39
R137A	91	6	94	1	1.17	0.07	1.72	0.02
R138A	90	6	94	1	1.10	0.12	1.73	0.13
E132Q	89	2	93	3	1.28	0.08	9.69	4.07
R137Q	92	2	93	7	1.14	0.03	2.08	0.35
R138Q	93	3	92	7	1.16	0.48	1.89	0.27
P130G	92	4	95	5	3.50	0.73	3.17	0.47
3LA	93	3	95	4	0.38	0.06	1.03	0.41

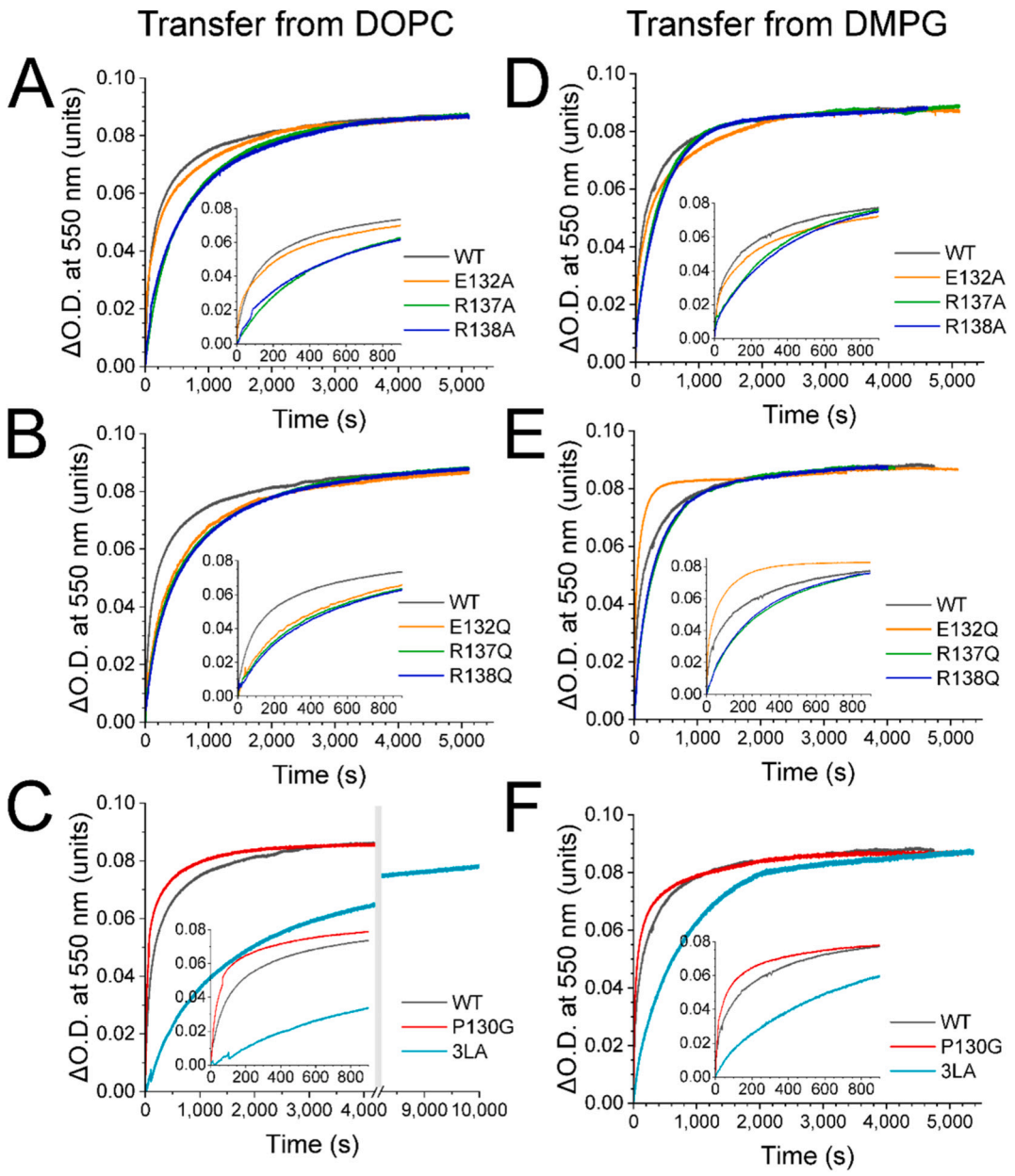

Fig. 4. Time course of AnaCTDH(CAN) holoprotein formation upon uptake of CAN from DOPC (A–C) and DMPG (D–F) liposomes by AnaCTDH wild-type and all sequence variants studied at 30 °C after addition of an excess of the respective apoprotein. The measurements were performed twice and the most typical results are presented. Note the time axis break in panel C (grey bar) to display the kinetics of the 3LA construct. The insets in each panel show the initial 900 s of the data on an expanded time scale.

membrane incorporation [39]. The increase in flexibility perhaps allows insertion from a wider range of angles apart from the perpendicular orientation, which could entail faster protein-lipid interaction, and, consequently, faster CAN uptake.

Finally, we interfered with overall hydrophobicity of the CTT by replacing the leucines Leu-133, Leu-134, and Leu-136 by alanines in construct 3LA. CAN transfer from both liposome types resulted in the slowest transfer of all sequence variants tested (Fig. 4C and F). The rate constants for extraction from DOPC and DMPG liposomes decreased by 81 % and 62 % respectively (Table 1). Since the three leucines define a hydrophobic interface of the CTT (Fig. 3A, upper panel), conceivable causes could be a reduced protein-lipid interaction due to the lower hydrophobicity, but also a decreased interaction to CAN, which would impede the sliding of CAN out of the membrane. The latter notion is supported by a study that focused, inter alia, on the Leu-136 residue by investigating the replacement for an aspartic acid (mutation L136D) (the amino acid numbering was adjusted herein to correspond to the sequence of the *all4940* gene, while the study cited [39] followed the numbering according to PDB structure 6FEJ). The decelerated kinetics observed in the mentioned study were explained by the challenging movement of CAN past the charged, less hydrophobic CTT of the L136D variant, as the CAN uptake (from membrane and from HCP1 holoprotein) and the CAN release (into HCP4 apoprotein) were slowed, regardless of the presence of the membrane [39]. However, since the 3LA triple mutation differentially affected CAN uptake kinetics depending on the liposome types tested, namely transfer from DOPC liposomes was significantly slower compared to uptake from DMPG liposomes, a lipid-dependent effect could be hypothesized: First, the reason could be a slightly different inclination angle of CAN within the membrane (due to the different membrane thickness) [55,56], which

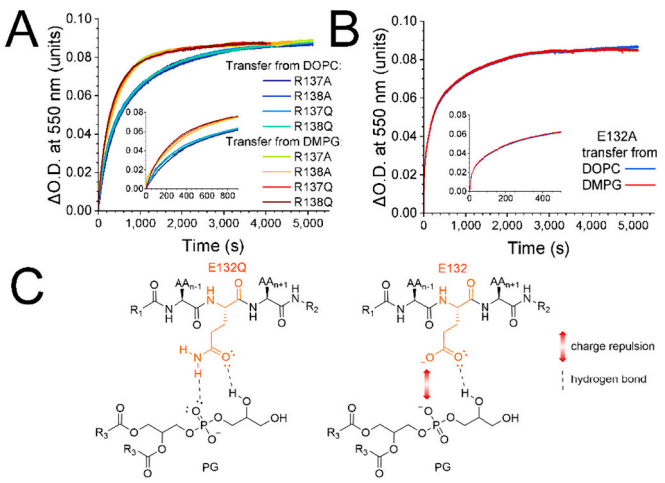

Fig. 5. Detailed consideration of individual mutations. Comparison of the time course of formation of AnaCTDH(CAN) holoproteins by arginine mutations (R137A, R137Q, R138A, R138Q) (A) and E132A (B), respectively. Insets in (A) and (B) show the data on an extended time scale. (C) Comparison of the models depicting the interaction between the PG head group and the Gln side chain in the E132Q variant or the Glu side chain in the WT protein (orange) based on hydrogen bonds and charge repulsion. "AA_{n-1}" and "AA_{n+1}" denote the preceding and following amino acid side chain.

would differentially affect carotenoid extraction in combination with the lower hydrophobicity of the CTT. Second, it is conceivable that the reduced hydrophobicity results in poorer interaction with the membrane especially with the hydrophobic fatty acid chains, which differ in chain lengths and fluidity in DOPC and DMPG. In total, the 3LA construct confirmed, nevertheless, that overall hydrophobicity is of high relevance for CAN transfer from artificial liposomes into AnaCTDH.

3.4. *Influence of point mutations in the CTT region of AnaCTDH on echinenone uptake*

The ECN transfer from liposomes into AnaCTDH to form the AnaCTDH(ECN) holoprotein is also spectroscopically detectable by absorbance change (Fig. 6) [36,37]. In previous work, we found that the kinetics of ECN uptake from liposomes into AnaCTDH is slower and the transfer yield is less efficient than with CAN [37], due to the lower stability of the ECN-coordinating AnaCTDH [34]. For this reason, only the transfer yield of the AnaCTDH(ECN) holoprotein was determined by decomposition of absorption spectra measured after 3 h at 30 °C, and after additional 21 h (i.e. 24 h in total) at room temperature (Table 2, Fig. 6). As already noted in previous studies, a loss of ECN was observed (e.g. due to bleaching, degradation, or precipitation), resulting in spectroscopically undetectable ECN fractions [37]. Furthermore, based on the results obtained in the CAN uptake experiments, chromophore-protein interaction of the holoproteins were assumed not to change in the case of ECN as well.

The maximum yield of AnaCTDH(ECN) holoprotein upon ECN transfer was about 50 % as described previously [37]. Two reasons are conceivable for the significantly lower transfer yield of ECN under the conditions of our experiments (large molar excess of apoprotein over carotenoid) compared to the case of AnaCTDH(CAN) formation. Briefly, one reason could be an equilibrium of ECN transfer from the membrane

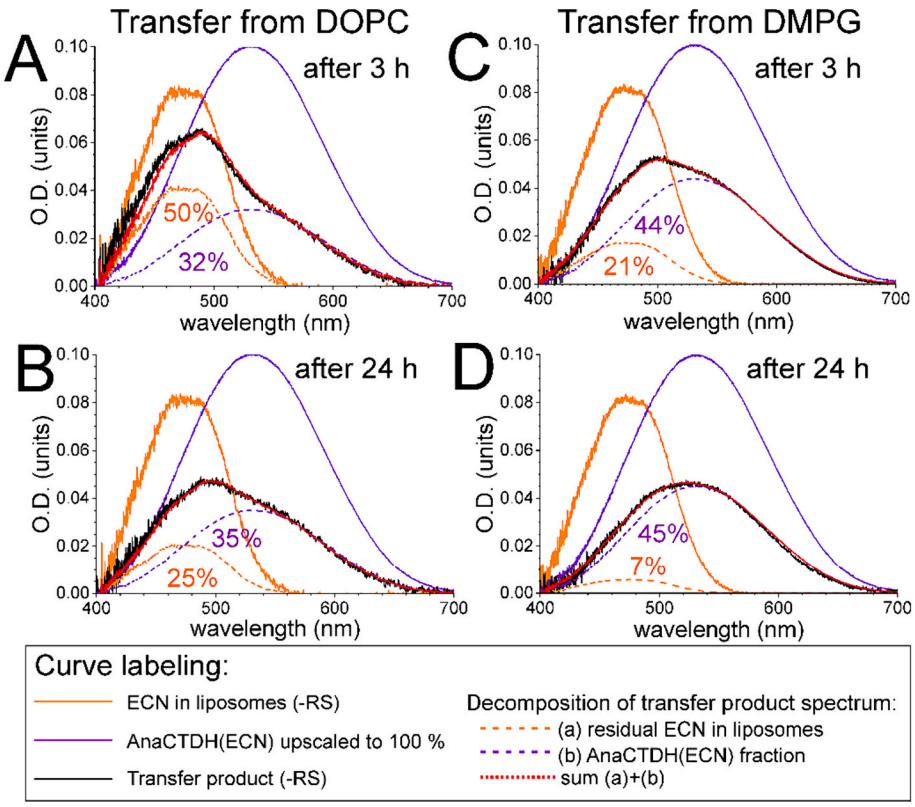

Fig. 6. Exemplary transfer of ECN from liposomes consisting of DOPC (A and B) and DMPG (C and D) into the AnaCTDH apoprotein mutant P130G after 3 h at 30 °C (A and C) and additional 21 h at room temperature (in total 24 h, B and D). The absorption spectra of ECN in the respective liposome preparation (orange curves) and the absorption spectra of the corresponding transfer product (black line) obtained after the addition of P130G are shown, in each case after subtraction the Rayleigh scattering background (-RS). For analysis, the spectrum of the transfer product was decomposed into a fraction of the ECN-loaded liposome preparation ((a), dashed orange line) and a fraction corresponding to the ECN-containing spectrum of the AnaCTDH holoprotein ((b), dashed purple line). The sum of the two fractions (a) and (b) is depicted as a red line and the spectrum of AnaCTDH(ECN) holoprotein, which should correspond to 100 % ECN transfer, is shown in purple.

Table 2
Comparison of transfer yields of AnaCTDH(ECN) holoprotein upon echinenone transfer from DOPC and DMPG liposomes by AnaCTDH WT and all sequence variants studied after 3 h at 30 °C and additional 21 h at room temperature. Results are expressed as mean value ± standard deviation given in juxtaposed columns ($n = 3$), with mean values presented as bars using the conditional formatting tool of Microsoft Excel.

Protein	Transfer yield from DOPC liposomes [%]				Transfer yield from DMPG liposomes [%]			
	3 h		24 h		3 h		24 h	
	Ø	σ	Ø	σ	Ø	σ	Ø	σ
WT	34	3	48	3	41	5	52	3
E132A	32	4	45	3	52	1	55	2
R137A	22	7	35	3	36	6	52	2
R138A	23	2	37	3	43	2	51	4
E132Q	24	1	50	4	47	4	54	3
R137Q	23	3	41	4	34	4	50	4
R138Q	24	3	44	4	42	4	53	3
P130G	35	3	34	1	44	7	40	5
3LA	4	1	17	2	35	4	51	6

into the protein and back. Presumably, ECN delivery from the protein to the liposome could be facilitated because the dimeric arrangement of AnaCTDH around an ECN molecule compared to the situation of diketolated CAN is less stable [31,34]. On the other hand, the orientation of the 4-ketolated β-ring of ECN in the membrane could limit the uptake into AnaCTDH [57], since for uptake, it is essential that the keto oxygen of ECN is directed toward the outside of the liposome in order to facilitate formation of hydrogen bonds to the conserved Tyr-26 and Trp-109 residues in AnaCTDH [31]. Since the fraction of ECN molecules exposing their keto oxygen atom toward the outer surface of the liposome should statistically be 50 %, it is reasonable to assume that ECN transfer is limited if rapid carotenoid flipping events do not take place within the time frame of the experiments.

Based on the ECN transfer yields obtained at different time points, conclusions regarding the ECN transfer efficiency of the AnaCTDH wild-type protein and all sequence variants studied were drawn. In general, ECN transfer from DOPC liposomes proceeds slower than from DMPG liposomes, as in the case of CAN transfer [37]. Furthermore, many similarities to the uptake of CAN were observed in the ECN uptake experiments by the various AnaCTDH constructs, but also some subtle differences. Considering the arginine substitutions by the mutations R137A, R137Q, R138A, and R138Q, all corresponding AnaCTDH variants exhibited lower transfer yields from DOPC liposomes compared to AnaCTDH wild-type after 3 h (Fig. 6A), which were almost independent of the mutation type and position as observed in the CAN transfer experiments. Due to the lower yields compared to wild-type protein, a weaker interaction with the lipid head group can be assumed. After additional 21 h at room temperature, there were indications that the Arg-137 substitutions generated slightly lower transfer yields compared to the Arg-138 substitutions within the same time span (Table 2). However, no significant difference within a mutation type could be detected with a significance threshold of $P < 0.05$ using the *t*-test. In ECN transfer from DMPG liposomes after 3 h at 30 °C, only the Arg-137 substitutions showed lower transfer yields compared to the wild-type protein. However, it is reasonable to assume that at an earlier time point, this would also have been observed for the Arg-138 mutations. Accordingly, the Arg-137 mutations also generated lower transfer yields compared to Arg-138 substitutions within 3 h. In this case, the one-tailed *t*-test revealed a significant difference between the constructs carrying mutations R137Q and R138Q with a significance threshold of $P < 0.05$. The hypothesis tested in the one-tailed *t*-test was that R137Q is a more critical factor for ECN uptake than R138Q [36]. For the mutants R137A and R138A, a significance on the $P > 0.05$ level (one-tailed *t*-test) could not be observed. Overall, evidence for the notion that Arg-137 is more important than Arg-138, e.g., as a membrane anchor, could be verified with statistical significance in one out of four cases (ECN transfer from DMPG liposomes by AnaCTDH carrying mutations R137Q). However, this does not preclude the notion, as each construct was tested only three times, with a quite large standard deviation in some cases.

In the ECN uptake experiments from DOPC liposomes after 3 h (Table 2), the AnaCTDH constructs carrying mutations of Glu-132 performed very similar as in CAN uptake. First, mutation E132Q has the same negative effect on the initial transfer rate, and, thus, on the lipid-protein interaction as the Arg-137/138 mutations in comparison to the wild-type protein. Second, mutation E132A produced transfer yields nearly identical to the wild-type. Similar to the arguments made about CAN uptake, this could have steric reasons compared to the E132Q substitution. In ECN uptake from DMPG liposomes after 3 h (Table 2), mutations E132A as well as E132Q produced larger transfer yields compared to the wild-type. The reason for this could be an improved lipid-protein interaction because a charge repulsion between the negatively charged head group of DMPG and the glutamic acid is absent (Fig. 5C). Since ECN uptake into AnaCTDH is generally slower than CAN uptake, the improved interaction with the liposome membrane appears to be of more importance in this case. Due to the different behaviour of the Glu-132 mutations with the two liposome types compared to AnaCTDH wild-type, this again supports the hypothesis of an anchor function of Glu-132 to the choline group of DOPC [36].

In addition to the acidic/basic amino acids of the CTT, the influence of the flexibility change by the P130G mutation was also investigated with ECN uptake experiments. The uptake from both types of liposomes clearly showed stagnation or even apparent reduction of the transfer yield between the measurements after 3 h and after 24 h (Table 2). As concluded from CAN uptake experiments, the increased flexibility of CTTs likely allows its incorporation into the membrane with a wider range of angles [39], leading to improved protein-lipid interaction. However, since the ECN-coordinating AnaCTDH dimer exhibits lower stability [34], the improved interaction most probably leads to a shifted equilibrium in favour of ECN delivery from AnaCTDH-P130G to liposomes despite the excess of apoprotein. Furthermore, the ECN transfer yields from DMPG liposomes were larger compared to DOPC at both measurement times, which can be attributed to the composition of the transfer product (Fig. 6). After decomposition of the Rayleigh scattering background-corrected spectra of the transfer products, a higher fraction of remaining ECN-loaded liposomes was observed in the uptake from DOPC liposomes compared to DMPG at both time points, even though this fraction decreased with time in both cases (Fig. 6). Therefore, the delivery of ECN from AnaCTDH-P130G back to DOPC liposomes was more pronounced compared to that to DMPG liposomes.

Finally, the influence of the overall hydrophobicity of the CTT by the

3LA triple-alanine mutation was examined with ECN uptake experiments. Comparable to CAN transfer, the AnaCTDH-3LA construct showed a significantly larger impact with DOPC liposomes. Specifically, the transfer yield from DMPG liposomes was only moderately reduced compared to the wild-type protein, in contrast to DOPC, from which the transfer yield dropped drastically to 4 % and 17 % after 3 h and 24 h, respectively (Table 2). As in the case of CAN, different reasons can account for this, which could perhaps even be interrelated. Briefly, the interaction between the less hydrophobic CTT and the membrane, precisely with the different fatty acid chains of DOPC and DMPG, could be reduced to a different extent. Secondly, the interaction between the less hydrophobic CTT and the hydrophobic ECN could be decreased, whereby the extraction from the membrane into the AnaCTDH becomes more difficult. The latter effect may possibly be affected to varying degrees by distinct incorporation angles of ECN in the two types of liposomes due to the different membrane thickness and fluidity [37,57]. Altogether, the overall hydrophobicity of the CTT structural element also exerts a decisive influence on the ECN transfer from artificial liposomes into AnaCTDH, especially in the case of DOPC liposomes.

4. Conclusions

The point mutations introduced into the CTT region of the AnaCTDH apoprotein offer valuable insights into the functions of specific amino acids during carotenoid uptake from artificial DMPG and DOPC liposomes. Thereby, the uptake of carotenoids canthaxanthin and echinenone is similarly affected by the point mutations.

The transfer experiments provide evidence supporting the hypothesis that Glu-132 has a membrane-anchoring effect on the PC lipids, specifically at the choline motif. The importance of this position within the CTT was highlighted by the strongly different effects of the variants on the extraction from the two liposome types. The transfer rate was uniformly reduced for all arginine variants of Arg-137 and Arg-138, depending on liposome type, indicating a weaker interaction, particularly with the lipid head group. Therefore, our study ascertained the importance of these arginines in carotenoid transfer. However, no significant superiority of Arg-137 over Arg-138 as a membrane anchor at the phosphate group of the lipid head group was established under the investigated conditions. The variation of Pro-130 strengthened the hypothesis that the CTT is oriented perpendicularly to the membrane and to the main AnaCTDH protein during membrane incorporation. Finally, the 3LA construct has provided confirmation that the overall hydrophobicity was crucial for carotenoid uptake, particularly in the case of DOPC. The results and methodological approaches described in this work can be of help for studies of carotenoid transfer processes mediated by other carotenoproteins. Of note, e.g. the P130G substitution accelerated carotenoid transfer, while other mutations slowed the rate down. Therefore, we anticipate substantial potential for engineering the carotenoid protein properties toward the requirements of particular applications.

Supplementary data to this article can be found online at https://doi.org/10.1016/j.bbabio.2024.149043.

CRediT authorship contribution statement

Kristina Likkei: Writing – review & editing, Writing – original draft, Visualization, Methodology, Investigation, Formal analysis. **Marcus Moldenhauer:** Writing – review & editing, Supervision, Methodology. **Neslihan N. Tavraz:** Writing – review & editing, Supervision, Resources, Methodology. **Nikita A. Egorkin:** Writing – review & editing, Methodology, Investigation, Formal analysis. **Yury B. Slonimskiy:** Writing – review & editing, Methodology, Investigation, Formal analysis. **Eugene G. Maksimov:** Writing – review & editing, Writing – original draft, Supervision, Project administration, Methodology, Funding acquisition, Conceptualization. **Nikolai N. Sluchanko:** Writing – review & editing, Writing – original draft, Supervision, Methodology, Funding acquisition, Formal analysis, Conceptualization. **Thomas Friedrich:** Writing – review & editing, Writing – original draft, Visualization, Validation, Supervision, Resources, Project administration, Funding acquisition, Formal analysis, Data curation, Conceptualization.

Declaration of competing interest

The authors declare that they have no known competing financial interests or personal relationships that could have appeared to influence the work reported in this paper.

Data availability

Data will be made available on request.

Acknowledgements

The authors acknowledge the support of the German Research Foundation (DFG grant no. FR1276/6-1). N.N.S., E.G.M., Y.B.S. and N.A.E. were partially supported by the Program of the Ministry of Science and Higher Education of the Russian Federation (075-15-2021-1354).

References

[1] A. Vershinin, Biological functions of carotenoids—diversity and evolution, Biofactors 10 (1999) 99–104.
[2] J. Manochkumar, C.G.P. Doss, H.R. El-Seedi, T. Efferth, S. Ramamoorthy, The neuroprotective potential of carotenoids in vitro and in vivo, Phytomedicine 91 (2021) 153676.
[3] B. Kulczyński, A. Gramza-Michałowska, J. Kobus-Cisowska, D. Kmiecik, The role of carotenoids in the prevention and treatment of cardiovascular disease – current state of knowledge, J. Funct. Foods 38 (2017) 45–65.
[4] C. Vílchez, E. Forján, M. Cuaresma, F. Bédmar, I. Garbayo, J.M. Vega, Marine carotenoids: biological functions and commercial applications, Mar. Drugs 9 (2011) 319–333.
[5] C.S. Foote, R.W. Denny, Chemistry of singlet oxygen. VII. Quenching by .beta-carotene, J. Am. Chem. Soc. 90 (1968) 6233–6235.
[6] H. Lokstein, G. Renger, J.P. Götze, Photosynthetic light-harvesting (antenna) complexes—structures and functions, Molecules 26 (2021) 3378.
[7] W. Stahl, H. Sies, Antioxidant activity of carotenoids, Mol. Asp. Med. 24 (2003) 345–351.
[8] T. Kay Holt, D.W. Krogmann, A carotenoid-protein from cyanobacteria, BBA-Bioenergetics 637 (1981) 408–414.
[9] D. Kirilovsky, Modulating energy arriving at photochemical reaction centers: orange carotenoid protein-related photoprotection and state transitions, Photosynth. Res. 126 (2015) 3–17.
[10] D. Kirilovsky, Photoprotection in cyanobacteria: the orange carotenoid protein (OCP)-related non-photochemical-quenching mechanism, Photosynth. Res. 93 (2007) 7–16.
[11] F. Muzzopappa, D. Kirilovsky, Photosynthesis|the orange carotenoid protein and the regulation of energy transfer in cyanobacteria, in: J. Jez (Ed.), Encyclopedia of Biological Chemistry III (Third Edition), Elsevier, Oxford, 2021, pp. 375–383.
[12] Y.P. Wu, D.W. Krogmann, The orange carotenoid protein of *Synechocystis* PCC 68031Publication No 153771, BBA-Bioenergetics 1322 (1997) 1–7.
[13] C.A. Kerfeld, M.R. Sawaya, V. Brahmandam, D. Cascio, K.K. Ho, C.C. Trevithick-Sutton, D.W. Krogmann, T.O. Yeates, The crystal structure of a cyanobacterial water-soluble carotenoid binding protein, Structure 11 (2003) 55–65.
[14] R.L. Leverenz, D. Jallet, M.-D. Li, R.A. Mathies, D. Kirilovsky, C.A. Kerfeld, Structural and functional modularity of the orange carotenoid protein: distinct roles for the N- and C-terminal domains in cyanobacterial photoprotection, Plant Cell 26 (2014) 426–437.
[15] C.A. Kerfeld, Structure and function of the water-soluble carotenoid-binding proteins of cyanobacteria, Photosynth. Res. 81 (2004) 215–225.
[16] A. Wilson, C. Punginelli, M. Couturier, F. Perreau, D. Kirilovsky, Essential role of two tyrosines and two tryptophans on the photoprotection activity of the Orange Carotenoid Protein, BBA-Bioenergetics 2011 (1807) 293–301.
[17] F. Muzzopappa, D. Kirilovsky, Changing color for photoprotection: the orange carotenoid protein, Trends Plant Sci. 25 (2020) 92–104.
[18] R.L. Leverenz, M. Sutter, A. Wilson, S. Gupta, A. Thurotte, C. Bourcier de Carbon, C.J. Petzold, C. Ralston, F. Perreau, D. Kirilovsky, C.A. Kerfeld, PHOTOSYNTHESIS: a 12 Å carotenoid translocation in a photoswitch associated with cyanobacterial photoprotection, Science 348 (2015) 1463–1466.
[19] E.G. Maksimov, N.N. Sluchanko, K.S. Mironov, E.A. Shirshin, K.E. Klementiev, G. V. Tsoraev, M. Moldenhauer, T. Friedrich, D.A. Los, S.I. Allakhverdiev, V. Z. Paschenko, A.B. Rubin, Fluorescent labeling preserving OCP photoactivity reveals its reorganization during the photocycle, Biophys. J. 112 (2017) 46–56.
[20] S. Gupta, M. Guttman, R.L. Leverenz, K. Zhumadilova, E.G. Pawlowski, C. J. Petzold, K.K. Lee, C.Y. Ralston, C.A. Kerfeld, Local and global structural drivers

for the photoactivation of the orange carotenoid protein, Proc. Natl. Acad. Sci. U. S. A. 112 (2015) E5567–E5574.
[21] H. Liu, H. Zhang, G.S. Orf, Y. Lu, J. Jiang, J.D. King, N.R. Wolf, M.L. Gross, R. E. Blankenship, Dramatic domain rearrangements of the cyanobacterial orange carotenoid protein upon photoactivation, Biochemistry 55 (2016) 1003–1009.
[22] C. Boulay, A. Wilson, S. D'Haene, D. Kirilovsky, Identification of a protein required for recovery of full antenna capacity in OCP-related photoprotective mechanism in cyanobacteria, Proc. Natl. Acad. Sci. U. S. A. 107 (2010) 11620–11625.
[23] H. Zhang, H. Liu, D.M. Niedzwiedzki, M. Prado, J. Jiang, M.L. Gross, R. E. Blankenship, Molecular mechanism of photoactivation and structural location of the cyanobacterial orange carotenoid protein, Biochemistry 53 (2014) 13–19.
[24] N.N. Sluchanko, Y.B. Slonimskiy, E.A. Shirshin, M. Moldenhauer, T. Friedrich, E. G. Maksimov, OCP–FRP protein complex topologies suggest a mechanism for controlling high light tolerance in cyanobacteria, Nat. Commun. 9 (2018) 3869.
[25] M. Moldenhauer, N.N. Sluchanko, N.N. Tavraz, C. Junghans, D. Buhrke, M. Willoweit, L. Chiappisi, F.-J. Schmitt, V. Vukojević, E.A. Shirshin, V. Y. Ponomarev, V.Z. Paschenko, M. Gradzielski, E.G. Maksimov, T. Friedrich, Interaction of the signaling state analog and the apoprotein form of the orange carotenoid protein with the fluorescence recovery protein, Photosynth. Res. 135 (2018) 125–139.
[26] R. López-Igual, A. Wilson, R.L. Leverenz, M.R. Melnicki, C. Bourcier de Carbon, M. Sutter, A. Turmo, F. Perreau, C.A. Kerfeld, D. Kirilovsky, Different functions of the paralogs to the N-terminal domain of the orange carotenoid protein in the cyanobacterium Anabaena sp PCC 7120, Plant Physiol. 171 (2016) 1852–1866.
[27] M.R. Melnicki, R.L. Leverenz, M. Sutter, R. López-Igual, A. Wilson, E.G. Pawlowski, F. Perreau, D. Kirilovsky, C.A. Kerfeld, Structure, diversity, and evolution of a new family of soluble carotenoid-binding proteins in cyanobacteria, Mol. Plant 9 (2016) 1379–1394.
[28] H. Bao, M.R. Melnicki, C.A. Kerfeld, Structure and functions of Orange Carotenoid Protein homologs in cyanobacteria, Curr. Opin. Plant Biol. 37 (2017) 1–9.
[29] C.A. Kerfeld, M.R. Melnicki, M. Sutter, M.A. Dominguez-Martin, Structure, function and evolution of the cyanobacterial orange carotenoid protein and its homologs, New Phytol. 215 (2017) 937–951.
[30] F. Muzzopappa, A. Wilson, V. Yogarajah, S. Cot, F. Perreau, C. Montigny, C. Bourcier de Carbon, D. Kirilovsky, Paralogs of the C-terminal domain of the cyanobacterial orange carotenoid protein are carotenoid donors to helical carotenoid proteins, Plant Physiol. 175 (2017) 1283–1303.
[31] D. Harris, A. Wilson, F. Muzzopappa, N.N. Sluchanko, T. Friedrich, E.G. Maksimov, D. Kirilovsky, N. Adir, Structural rearrangements in the C-terminal domain homolog of Orange Carotenoid Protein are crucial for carotenoid transfer, Commun. Biol. 1 (2018) 125.
[32] M.A. Dominguez-Martin, M. Hammel, S. Gupta, S. Lechno-Yossef, M. Sutter, D. J. Rosenberg, Y. Chen, C.J. Petzold, C.Y. Ralston, T. Polívka, C.A. Kerfeld, Structural analysis of a new carotenoid-binding protein: the C-terminal domain homolog of the OCP, Sci. Rep. 10 (2020) 15564.
[33] E.G. Maksimov, G.Y. Laptev, D.S. Blokhin, V.V. Klochkov, Y.B. Slonimskiy, N. N. Sluchanko, T. Friedrich, C.-F. Chang, V.I. Polshakov, NMR resonance assignment and backbone dynamics of a C-terminal domain homolog of orange carotenoid protein, Biomol. NMR Assign. 15 (2021) 17–23.
[34] Y.B. Slonimskiy, F. Muzzopappa, E.G. Maksimov, A. Wilson, T. Friedrich, D. Kirilovsky, N.N. Sluchanko, Light-controlled carotenoid transfer between water-soluble proteins related to cyanobacterial photoprotection, FEBS J. 286 (2019) 1908–1924.
[35] M. Moldenhauer, N.N. Sluchanko, D. Buhrke, D.V. Zlenko, N.N. Tavraz, F.-J. Schmitt, P. Hildebrandt, E.G. Maksimov, T. Friedrich, Assembly of photoactive orange carotenoid protein from its domains unravels a carotenoid shuttle mechanism, Photosynth. Res. 133 (2017) 327–341.
[36] E.G. Maksimov, A.V. Zamaraev, E.Y. Parshina, Y.B. Slonimskiy, T.A. Slastnikova, A. A. Abdrakhmanov, P.A. Babaev, S.S. Efimova, O.S. Ostroumova, A.V. Stepanov, E. A. Slutskaya, A.V. Ryabova, T. Friedrich, N.N. Sluchanko, Soluble cyanobacterial carotenoprotein as a robust antioxidant nanocarrier and delivery module, Antioxidants 9 (2020) E869.
[37] K. Likkei, M. Moldenhauer, N.N. Tavraz, E.G. Maksimov, N.N. Sluchanko, T. Friedrich, Lipid composition and properties affect protein-mediated carotenoid uptake efficiency from membranes, BBA-Biomembranes 1866 (2023) 184241.
[38] E.G. Maksimov, N.N. Sluchanko, Y.B. Slonimskiy, K.S. Mironov, K.E. Klementiev, M. Moldenhauer, T. Friedrich, D.A. Los, V.Z. Paschenko, A.B. Rubin, The unique protein-to-protein carotenoid transfer mechanism, Biophys. J. 113 (2017) 402–414.
[39] D. Harris, F. Muzzopappa, F. Glaser, A. Wilson, D. Kirilovsky, N. Adir, Structural dynamics in the C terminal domain homolog of orange carotenoid protein reveals residues critical for carotenoid uptake, BBA-Bioenergetics 1861 (2020) 148214.
[40] A. Mezzetti, M. Alexandre, A. Thurotte, A. Wilson, M. Gwizdala, D. Kirilovsky, Two-step structural changes in orange carotenoid protein photoactivation revealed by time-resolved Fourier transform infrared spectroscopy, J. Phys. Chem. B 123 (2019) 3259–3266.
[41] P.E. Konold, I.H.M. van Stokkum, F. Muzzopappa, A. Wilson, M.-L. Groot, D. Kirilovsky, J.T.M. Kennis, Photoactivation mechanism, timing of protein secondary structure dynamics and carotenoid translocation in the Orange Carotenoid Protein, J. Am. Chem. Soc. 141 (2019) 520–530.
[42] J.B. Rose, J.A. Gascón, M. Sutter, D.I. Sheppard, C.A. Kerfeld, W.F. Beck, Photoactivation of the orange carotenoid protein requires two light-driven reactions mediated by a metastable monomeric intermediate, Phys. Chem. Chem. Phys. 25 (2023) 33000–33012.
[43] S. Niziński, I. Schlichting, J.-P. Colletier, D. Kirilovsky, G. Burdzinski, M. Sliwa, Is orange carotenoid protein photoactivation a single-photon process? Biophys. Rep. 2 (2022) 100072.
[44] E.G. Maksimov, M. Moldenhauer, E.A. Shirshin, E.A. Parshina, N.N. Sluchanko, K. E. Klementiev, G.V. Tsoraev, N.N. Tavraz, M. Willoweit, F.-J. Schmitt, J. Breitenbach, G. Sandmann, V.Z. Paschenko, T. Friedrich, A.B. Rubin, A comparative study of three signaling forms of the orange carotenoid protein, Photosynth. Res. 130 (2016) 389–401.
[45] V.A. Anashkin, Y.V. Bertsova, A.M. Mamedov, M.D. Mamedov, A.M. Arutyunyan, A.A. Baykov, A.V. Bogachev, Engineering a carotenoid-binding site in Dokdonia sp PRO95 Na+-translocating rhodopsin by a single amino acid substitution, Photosynth. Res. 136 (2018) 161–169.
[46] N. Steube, M. Moldenhauer, P. Weiland, D. Saman, A. Kilb, A.A. Ramírez Rojas, S. G. Garg, D. Schindler, P.L. Graumann, J.L.P. Benesch, G. Bange, T. Friedrich, G.K. A. Hochberg, Fortuitously compatible protein surfaces primed allosteric control in cyanobacterial photoprotection, Nat. Ecol. Evol. 7 (2023) 756–767.
[47] M. Golub, M. Moldenhauer, F.-J. Schmitt, A. Feoktystov, H. Mändar, E. Maksimov, T. Friedrich, J. Pieper, Solution structure and conformational flexibility in the active state of the orange carotenoid protein: part I small-angle scattering, J. Phys. Chem. B 123 (2019) 9525–9535.
[48] J.R. Silvius, Thermotropic phase transitions of pure lipids in model membranes and their modifications by membrane proteins, in: Lipid-Protein Interactions, John Wiley & Sons Inc., New York, 1982, pp. 239–281.
[49] L. Šturm, N. Poklar Ulrih, Basic methods for preparation of liposomes and studying their interactions with different compounds, with the emphasis on polyphenols, Int. J. Mol. Sci. 22 (2021) 6547.
[50] G. Britton, S. Liaaen-Jensen, H. Pfander, Carotenoids Handbook, Springer Basel AG, 2004.
[51] Y.B. Slonimskiy, E.G. Maksimov, E.P. Lukashev, M. Moldenhauer, C.M. Jeffries, D. I. Svergun, T. Friedrich, N.N. Sluchanko, Functional interaction of low-homology FRPs from different cyanobacteria with Synechocystis OCP, BBA-Bioenergetics 2018 (1859) 382–393.
[52] D. Svergun, C. Barberato, M.H.J. Koch, CRYSOL – a program to evaluate X-ray solution scattering of biological macromolecules from atomic coordinates, J. Appl. Crystallogr. 28 (1995) 768–773.
[53] H.B. Bull, K. Breese, Surface tension of amino acid solutions: a hydrophobicity scale of the amino acid residues, Arch. Biochem. Biophys. 161 (1974) 665–670.
[54] C.N. Pace, J.M. Scholtz, A helix propensity scale based on experimental studies of peptides and proteins, Biophys. J. 75 (1998) 422–427.
[55] W. Grudzinski, L. Nierzwicki, R. Welc, E. Reszczynska, R. Luchowski, J. Czub, W. I. Gruszecki, Localization and orientation of xanthophylls in a lipid bilayer, Sci. Rep. 7 (2017) 9619.
[56] A. Sujak, J. Gabrielska, J. Milanowska, P. Mazurek, K. Strzałka, W.I. Gruszecki, Studies on canthaxanthin in lipid membranes, BBA-Biomembranes 1712 (2005) 17–28.
[57] A.N. Semenov, D.A. Gvozdev, D.V. Zlenko, E.A. Protasova, A.R. Khashimova, E. Y. Parshina, A.A. Baizhumanov, N.Y. Lotosh, E.E. Kim, Y.N. Kononevich, A. A. Pakhomov, A.A. Selishcheva, N.N. Sluchanko, E.A. Shirshin, E.G. Maksimov, Modulation of membrane microviscosity by protein-mediated carotenoid delivery as revealed by time-resolved fluorescence anisotropy, Membranes 12 (2022) 905.